Two-stage Bayesian model to evaluate the effect of air pollution on chronic respiratory diseases using drug prescriptions

Marta Blangiardo[a,], Francesco Finazzi[b], Michela Cameletti[b]

[a] *MRC Centre for Environment and Health, Department of Epidemiology and Biostatistics, Imperial College London, UK*
[b] *Department of Management, Economics and Quantitative Methods, University of Bergamo, Italy*

Abstract

Exposure to high levels of air pollutant concentration is known to be associated with respiratory problems which can translate into higher morbidity and mortality rates. The link between air pollution and population health has mainly been assessed considering air quality and hospitalization or mortality data. However this approach limits the analysis to individuals characterized by severe conditions. In this paper we evaluate the link between air pollution and respiratory diseases using general practice drug prescriptions for chronic respiratory diseases, which allow to draw conclusions based on the general population.

We propose a two-stage statistical approach: in the first stage we specify a space-time model to estimate the monthly NO_2 concentration integrating several data sources characterized by different spatio-temporal resolution; in the second stage we link the concentration to the β_2-agonists prescribed monthly by general practices in England and we model the prescription rates through a small area approach.

Keywords: Bayesian model, INLA, COSP, General Practice

Email address: m.blangiardo@imperial.ac.uk (Marta Blangiardo)

1. Introduction

Exposure to high levels of air pollutant concentration is known to be associated with respiratory problems which can translate into higher morbidity and mortality rates. Short term and long term effects have been documented, with a scientific literature increasing exponentially since the London great smog in 1952 and the following Clean Air Act of 1955 in the US and 1956 in the UK (Schwartz and Marcus, 1990; Dockery et al., 1993; Atkinson et al., 2014; Rushworth et al., 2014), with particular focus on cardiovascular and respiratory diseases (Brunekreef and Holgate, 2002; Künzli, 2012; Schikowski et al., 2005; Lanki et al., 2006; Brook et al., 2010).

Asthma and chronic obstructive pulmonary disease (COPD) are the two main respiratory diseases which cause heavy social and economic burden worldwide (WHO, 2012). It is estimated that the number of people who are suffering from asthma was 334 million around the world in 2014 and this number is projected to elevate to 400 million by the year 2025 (Masoli et al., 2004). According to the latest World Health Organisation (WHO) estimation, 64 million people are currently suffering from COPD and there are 3 million deaths attributable to this condition; they predict that COPD will become the third leading cause of death worldwide by 2030 (Vos et al., 2015). As asthma and COPD are both long-term conditions, they can be controlled by regular medication. According to the recent report of the Office for National Statistics (ONS), the drugs prescribed for controlling these conditions have experienced a rapid increase in recent years, so it becomes more and more important to carry out epidemiological surveillance and risk assessment of such diseases, with the aim of guiding decision making for control and prevention (Prescribing and Primary Care Health and Social Care Information Centre, 2014).

Historically, administrative datasets such as Hospital Episode Statistics (HES) or Mortality registries have been used for this purpose and the nature of these registries implies that only individuals characterized by a severe condition of the diseases are included in the analysis. Alternatively data on drug prescriptions from general practices (GPs) allows to change the perspective to primary care and to focus on the general population instead of restricting the analysis to severe cases.

The strength and validity of GP prescription data have been proven by several studies for different diseases using diverse study designs (Hansell et al., 1999; Katz et al., 2010; Jick et al., 2003), for example evaluating

the risk of cardiovascular diseases (Osborn et al., 2007; Clayton et al., 2008), monitoring the use of antibiotics for respiratory diseases (Howie et al., 1971; Petersen et al., 2007) and identifying asthmatic children through GP prescription database (Moth et al., 2007). A few studies have used salbutamol prescribing data in respiratory diseases surveillance. Vegni et al. (2005) used a Poisson regression model to study how the respiratory drug dispensation is linked to the air pollution effect of total suspended particles and suggested that respiratory drug prescribing data are a good indicator of air pollution. Naureckas et al. (2005) used short acting β_2-agonists (SABA) prescription as an indicator of asthma attributable hospital admissions and found a significantly positive relationship between SABA prescription and hospital admissions at area level. A study by Laurent et al. (2009) suggested that SABA sales would increase with the elevated concentration of air pollution factors such as NO_2, PM_{10} and O_3. Sofianopoulou et al. (2013) used primary care data to investigate the association between respiratory prescription, social economic status and PM_{10} and found a small but positive increase in prescriptions for an increase in air pollution.

In all these studies, SABA prescription data were limited to specific regions (Como, Italy for Vegni et al., 2005; Newcastle and North Tyneside for Sofianopoulou et al., 2013; Strasbourg region in France for Laurent et al., 2009), while to the best of our knowledge no previous study has focused on an entire country at a small area level.

In this paper we propose to evaluate the link between air pollution and respiratory diseases through a two stage approach: in the first stage we develop a spatio-temporal model for Nitrogen Dioxide (NO_2) as measure of air pollution. The model considers that monthly NO_2 concentrations are realizations of a continuous spatial process that changes in time with an autoregressive dynamics; in addition it includes some covariates characterized by a different spatial resolution, ultimately aiming at prediction of NO_2 at a different spatial resolution. This leads to the change of support problem (COSP, Gotway and Young, 2002; Gelfand et al., 2010), a crucial issue in environmental modeling and health risk assessment. In the literature several solutions have been identified to deal with the COSP, mainly by means of hierarchical models; see for example the Bayesian melding of Fuentes and Raftery (2005), the spatio-temporal downscaler of Berrocal et al. (2010a), the joint modelling of point and grid spatio-temporal data by Sahu et al. (2010) and the Bayesian 2-Stage Space-Time Mixture Modeling of Lawson et al. (2012). A critical point concerning COSP regards the computational

costs, which can become prohibitive in case of massive data sets or complex models, giving rise to the so called *big n problem* (Lasinio et al., 2013). In this work we propose a computationally efficient solution to the COSP by adopting the Integrated Nested Laplace Approximation (INLA) approach developed by Rue et al. (2009) and implemented in the `R-INLA` package (`http://www.r-inla.org/`). We use the first stage model to perform point-to-area NO_2 prediction, so that the pollutant concentration estimates are available at the same spatio-temporal resolution of the drug prescriptions. At the second stage, the NO_2 concentration is linked to the prescription rates in a small area approach, taking into account potential confounders.

An additional feature of our modelling framework is that we move away from the standard public health approach, where the exposure estimated at the first stage is plugged in the second stage without taking its uncertainty into account (Rushworth et al., 2014; Lee and Sarran, 2015; Huang et al., 2015); instead we consider the entire NO_2 posterior distribution from the first stage and feed it forward into the health model. We compare the results from this model with the *naive* one, that plugs in the mean from the NO_2 distribution into the second stage model.

The rest of the paper is structured as follows. Section 2 presents the data considered in this work. Section 3 introduces the first stage statistical model which is used to obtain NO_2 estimates at the area level for a monthly temporal resolution, while Section 4 describes the second stage statistical model used to link exposure with the health data. After a short introduction in Section 5 of the INLA approach adopted for Bayesian inference in spatial statistics, results and main findings are reported in Section 6, while discussion points and concluding remarks are given in Section 7.

2. Exploratory data analysis

2.1. Drug prescription data

Drug prescribing data are released by the English National Health Service (NHS) for all the GPs in England and all the drugs and are available from `https://data.gov.uk/`. The database includes around 11,000 practices and 30,000 drugs with around 112 million drug items prescribed and redeemed each month. For each general practice the number of drug items prescribed monthly are provided. In this work, prescribing data regarding the following drugs based on short acting β_2-agonists are considered: Salbutamol 100mcg, Ventolin 100mcg and Clenil Modulite 100mcg, accounting for

around 96% of all β_2-agonists prescriptions in England (Sofianopoulou et al., 2013). Additionally the geographic coordinates of each GP are available. We limit the analysis to the 8,003 practices where information on the registered population is available to the period from August 2010 to November 2012.

Figure 1 shows the space and time rates of β_2-agonists prescriptions, calculated as the ratio between observed and expected prescription assuming the whole of England as standard population. As a geographical unit we consider the clinical commissioning groups (CCG), which are organizations of GPs in the same area and that are responsible to provide health and care services to patients. From the figure a spatial variability is visible, with more prescriptions in the north, north-est and in the south-west corner of the country. A temporal variability can also be appreciated, with an increase in prescription for early spring, which might be explained by allergies, and late autumn/early winter, which could relate to infections.

2.2. NO_2 concentration data

Data about Nitrogen Dioxide (NO_2, in $\mu g/m^3$) concentration are available through the OpenAir project (Carslaw and Ropkins, 2012) and the related `R` package `openair` (Carslaw and Ropkins, 2015). In particular, we consider the daily NO_2 data for the period August 2010 - November 2012 available from the UK Automatic Urban and Rural Network (AURN), the King's College London's London Air Quality Network (KCL) and the European Air quality dataBase (AIRBASE). We excluded kerbside and roadside stations and considered only sites with at least 75% of data. The final dataset comprises 44 stations for which monthly NO_2 mean concentration and coordinates are available (see Figure 2). The NO_2 monthly time series reported in Figure 3 show, as expected, higher pollutant concentration in the cold season; moreover, most of the stations are characterized by a similar temporal pattern.

2.3. NO_2 baseline data

As NO_2 stations are quite sparse over England and there are some areas with no monitoring sites, we integrate these data with the annual NO_2 concentration obtained combining a numerical model (ADMS-Urban) and land use regression (Gulliver et al., 2013). These data, while being constant in time, are defined at a very high spatial resolution given by the Lower Super Output Area (LSOA) geography (32,844 areas); we consider here 2009 as this is the latest year when concentration at such a fine resolution is available and use it to represent the NO_2 baseline level. From the map in Figure

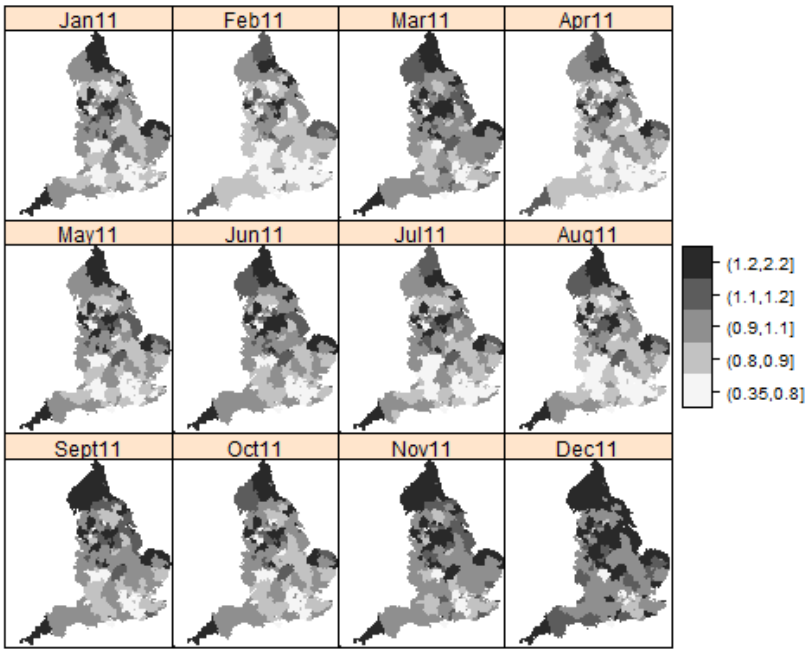

Figure 1: Map of monthly prescription rates for β_2-agonists in England for 2011. The spatial unit considered is the Clinical Commissioning Group (CCG).

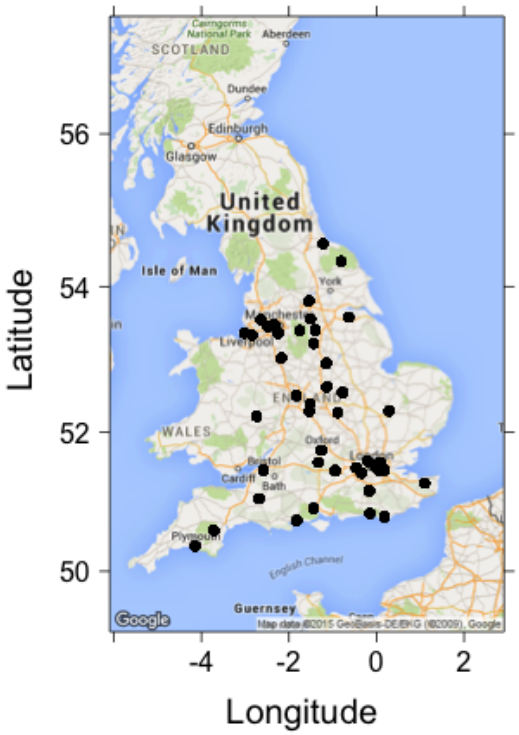

Figure 2: Map of NO_2 monitoring stations in England.

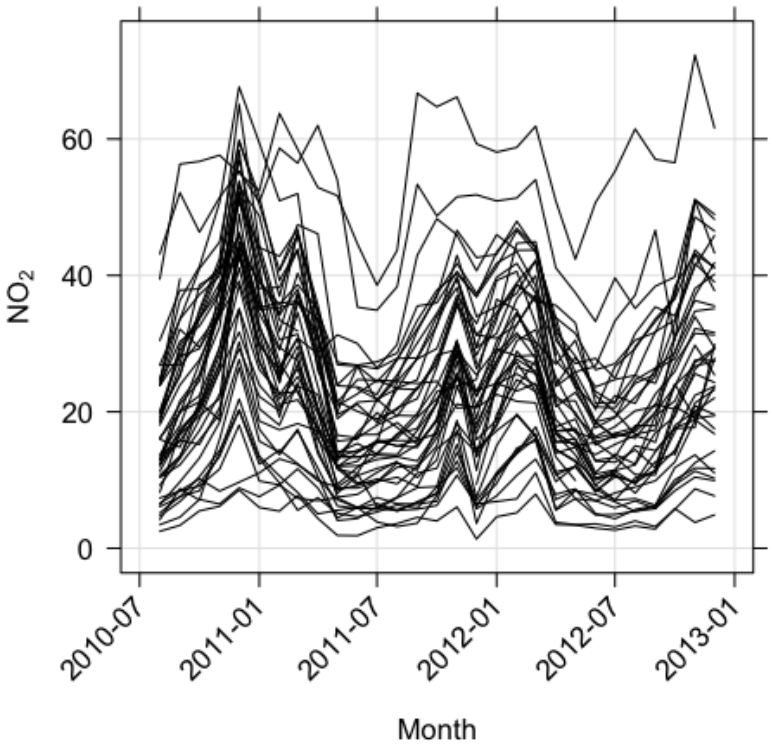

Figure 3: NO_2 concentration (in $\mu g/m^3$) monthly time series for the 44 stations in England (August 2010 - November 2012).

4 it is possible to identify some zones with high levels of NO_2 concentration located around the main urban areas, e.g. London, Manchester, Liverpool and Newcastle.

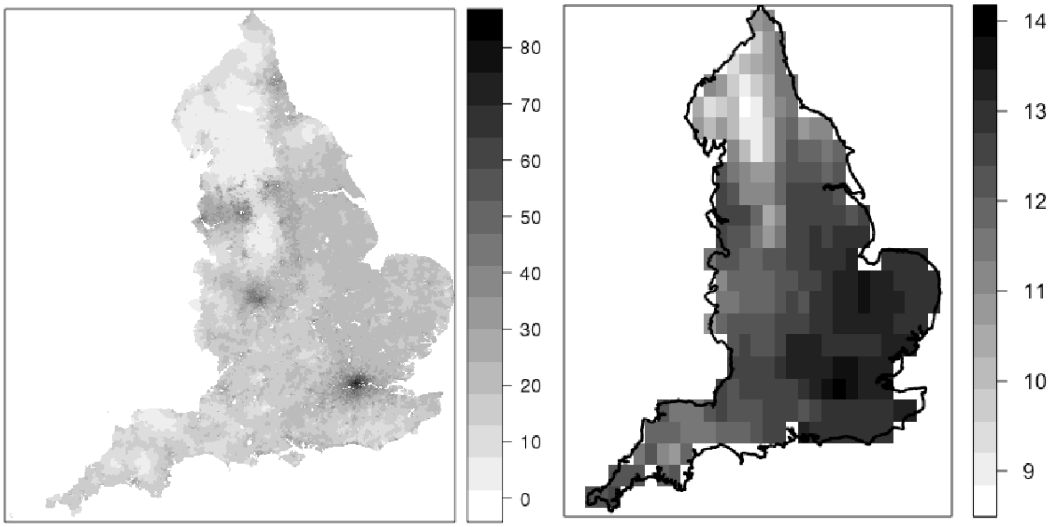

Figure 4: Map of NO_2 baseline level (in $\mu g/m^3$) for 2009 with LSOA resolution (left) and map of mean temperature in C° for May 2011 on a 0.25 degree regular latitude-longitude grid.

2.4. Temperature data

To take into account the NO_2 seasonality shown in Figure 3 we consider daily temperature data, which are made available on a 0.25 degree regular latitude-longitude grid (covering Europe and the Mediterranean) by the European Climate Assessment & Dataset project (Haylock et al., 2008) (`http://www.ecad.eu/`). For this work, we compute monthly mean averages for the period of interest (August 2010 - November 2012) and for the grid cells covering England (see for example Figure 4). As expected, the average temporal correlation between NO_2 concentration and temperature, computed by assigning to each monitoring station the temperature value of the closest cell, is negative and moderate (-0.42).

2.5. Confounders

Several factors can influence the relationship between air pollution and drug prescribing rates. For this reason in the epidemiological analysis at the second stage of the modelling framework we include the known confounders available from different sources. From the GP datasets the population by age and sex registered to each practice is available and we calculate the % of active population (between 14 and 64 years old) and the % of males. From the Health and Social Care Information Centre we obtained asthma and chronic obstructive pulmonary disease prevalence at the GP level and for the period August 2010 - November 2012 (`http://www.hscic.gov.uk/catalogue/PUB05756`). Finally, from the Department for Communities and Local Government (`https://www.gov.uk/government/collections/english-indices-of-deprivation`) we downloaded the multiple deprivation index (IMD) at the LSOA level and linked each practice to the corresponding area.

3. First stage: spatio-temporal NO_2 model

The first stage concerns the modeling of NO_2 monthly concentration available at the 44 monitoring sites, by integrating also temperature and NO_2 baseline data. To deal with the spatial misalignment of the considered datasets, we associate with each NO_2 station the temperature and NO_2 baseline value of the nearest grid cell or area (see e.g. Berrocal et al., 2010b; Zidek et al., 2011). The spatio-temporal model we specify here is widely adopted in the air quality literature thanks to its flexibility in modeling relevant covariates as well as correlation in space and time (Fassò and Finazzi, 2011; Cocchi et al., 2007; Cameletti et al., 2011; Sahu, 2011). Moreover, it has been already implemented in `R-INLA` and validated by Cameletti et al. (2013).

Let y_{it} denote the NO_2 concentration (square root transformed to ensure normality) measured at station located at site s_i ($i = 1, \ldots, 44$) and month $t = 1, \ldots, 28$. We assume the following distribution for the observations

$$y_{it} \sim \text{Normal}(\eta_{it}, \sigma_e^2)$$

with linear predictor given by

$$\eta_{it} = \beta_0 + \beta_1 \text{Temp}_{it} + \beta_2 \text{NO2baseline}_i + \omega_{it}, \quad (1)$$

where $\boldsymbol{\beta} = \{\beta_0, \beta_1, \beta_2\}$ are the fixed effects. The term ω_{it} refers to the latent spatio-temporal process which changes in time with first order autoregressive dynamics with coefficient a and spatially correlated innovations:

$$\omega_{it} = a\omega_{i(t-1)} + \xi_{it},$$

for $t = 2, \ldots, 28$, with $|a| < 1$ and ω_{i1} deriving from the stationary distribution Normal$(0, \sigma_\omega^2/(1-a^2))$. In the previous equation ξ_{it} is a zero-mean Gaussian Field (GF) defined by the following spatio-temporal covariance function

$$\text{Cov}\left(\xi_{it}, \xi_{ju}\right) = \begin{cases} 0 & \text{if} \quad t \neq u \\ \mathcal{C}(s_i, s_j) & \text{if} \quad t = u \end{cases},$$

where $\mathcal{C}(s_i, s_j)$ is the Matérn covariance function (Cressie and Wikle, 2011)

$$\mathcal{C}(s_i, s_j) = \frac{\sigma_\omega^2}{\Gamma(\lambda)2^{\lambda-1}} \left(\kappa||s_i - s_j||\right)^\lambda K_\lambda \left(\kappa||s_i - s_j||\right)$$

depending on the Euclidean spatial distance $h = ||s_i - s_j|| \in \mathbb{R}$, the spatial variance σ_ω^2 and the scaling term κ. The term $K_\lambda(\cdot)$ denotes the modified Bessel function of second kind and order $\lambda > 0$. Lindgren et al. (2011) proposed an empirically derived definition for the range $\rho = \sqrt{8\lambda}/\kappa$, interpreted as the distance at which the spatial correlation is close to 0.1 for each $\lambda \geq 1/2$.

Model estimation and prediction is performed in a Bayesian setting using the INLA-SPDE approach described in Section 5. Note that in `R-INLA` the smoothness parameter λ, which is usually kept fixed to ensure model identifiability, is by default equal to 1; in addition the SPDE parameters are represented as $\log(\tau) = \theta_1$ (τ is related to the variance through the relationship $\sigma_\omega^2 = 1/(4\pi\kappa^2\tau^2)$) and $\log(\kappa) = \theta_2$, with θ_1 and θ_2 being given independent Normal(0,1) prior distributions (for more details see Blangiardo and Cameletti, 2015). Moreover, weakly informative Normal priors centered on 0 and with a small precision equal to 0.01 are specified for the fixed effects in Equation (1).

As we are interested in predicting the NO_2 concentration - represented by the linear predictor in (1) - at the Middle Super Output Area level (MSOA) - for inclusion in the second model stage (see Section 4), we perform this change of support from points to areas in two steps: first the posterior distribution of NO_2 concentration is obtained for a regular grid and for all the time points (in particular we use the grid described in Section 2.4). This task can be

easily achieved using the SPDE approach, which provides an approximation of the spatial process over all the considered spatial domain. Second, for a given time point t and area B_k, we compute a linear combination of the NO_2 posterior distributions η_{jt} available at the grid cells $\mathcal{S}_j$ which have an intersection with area B_k:

$$\mathrm{NO}_{2B_kt} = \sum_{\mathcal{S}_j} \eta_{jt}\Delta_j, \tag{2}$$

where $\Delta_j = |\mathcal{S}_j \cap B_k|$ is the weight identifying the proportion of the j-th grid cell overlapping with the MSOA B_k. Note that the MSOA spatial resolution has been chosen to approximate the GP catchment areas; in addition it is a relatively small area with a population on average around 10,000 individuals, but at the same time it ensures computational tractability (there are 6790 MSOA in England to be predicted over 28 months).

4. Second stage: health data model

The NO_2 concentration predicted at the MSOA level from the first stage model in (2) is linked to the GP prescription data in the second stage. We assume a Poisson distribution for the number of prescriptions O_{kt} for practice k ($k = 1, \ldots, 8003$) at month t ($t = 1, \ldots, 28$):

$$O_{kt} \sim \mathrm{Poisson}(\theta_{kt}\mathrm{E}_{kt})$$

with E_{kt} indicating the number of expected prescriptions for each practice and each month considering the whole of England as the standard region, while the typical log-linear model is specified on the risk θ_{kt}

$$\log(\theta_{kt}) = \gamma_0 + \boldsymbol{x}_{kt}^T\boldsymbol{\gamma} + U_k + v_{c_k} + u_{c_k} + \zeta_t, \tag{3}$$

where γ_0 is the intercept and represents the average prescription rate across England, $\boldsymbol{\gamma} = \{\gamma_1, \ldots, \gamma_P\}$ identifies the covariate effects including the exposure of interest (NO_{2B_kt}) from the MSOA where each GP is located and the confounders (age, sex, prevalence of COPD, prevalence of asthma, quartiles of deprivation). Note that the inclusion of COPD and asthma prevalence adjusts for the *baseline* prescription rate due to underlying cases of obstructive respiratory diseases at each GP and allows to pick up the effect of air pollution on the prescribing rates for new cases or for exacerbated ones. We

include a random effect at the GP level ($U_k \sim \text{Normal}(0, \tau_U)$, with a non informative prior on τ_U) to consider the effect of unmeasured confounders at that level.

As the CCGs are man-made organisations which take decisions on primary care strategies, it is reasonable to assume that they influence the prescribing behaviour at GP level. To take this into account we include a Besag-York-Mollie specification (BYM, Besag et al., 1991) for CCGs ($c = 1, \ldots, 211$), assuming $v_c \sim \text{Normal}(0, \tau_v)$ and a conditionally autoregressive structure for u_c:

$$u_c \mid u_{-c} \sim \text{Normal}\left(\frac{\sum_{j \in D_c} u_j}{n_{D_c}}, (n_{D_c}\tau_u)\right)$$

where D_c is the set of neighbouring areas for CCG c and n_{D_c} is its total number of neighbours.

In this paper we specify a modified version of the BYM as proposed by MacNab (2011) and Simpson et al. (2015), and recently implemented in `R-INLA`. This prior specification relaxes the assumption of independence between u_c and v_c and at the same time considers a standardised marginal variance so that the hyperprior does not depend on the neighbouring structure and it is transferable and comparable across studies based on different neighbouring structures (Simpson et al., 2015). Thus the specification presented in (3) becomes the following

$$\log(\theta_{kt}) = \gamma_0 + \boldsymbol{x}_{kt}^T\boldsymbol{\gamma} + U_k + \zeta_t + \frac{1}{\sqrt{\tau}}\left(\sqrt{1-\phi}v_{c_k} + \sqrt{\phi}u^*_{c_k}\right) \tag{4}$$

where u_c^* is a modified random effect which has a marginal precision equal to 1 and v_c has a Normal distribution centered on 0 with precision equal to 1. Both random effects are specified at the CCG level and are driven by two hyperparameters: a precision τ on which a Gumbel distribution is specified and a scale parameter ϕ which governs the proportion of variability due to the local spatial dependency or to the global smoothing. This can also be interpreted in terms of penalised complexity, assuming that ϕ is different from 0 if the data provide evidence of a spatial pattern which cannot be explained by the simpler random effect $\boldsymbol{v}$. The prior on ϕ is given by an exponential distribution truncated between 0 and 1.

As the data span over 28 months ζ_t is included to account for the temporal variation in prescriptions and is modelled as an autoregressive of order 1,

NO_2 modelling	**NO_2 prediction**	**GP model**	**Residuals**
Points: 44 Monitors LSOA: baseline NO_2 at 2009 Grid: Temperature	 MSOA	Points: Prescriptions Points: Confounders 8003 general practices 28 months	Clinical Commissioning Group (CCG): Spatially structured and unstructured effects Practice level: unstructured effect
Why chosen			
Data availability	To approximate GP catchment areas	To allow variability across GPs to be considered	To account for clustering (CCG) and GP level variability

Table 1: Summary of the different spatial resolutions used in the modelling framework.

assuming that each time point depends only on the previous one in the time series as follows:

$$\zeta_t = b\zeta_{t-1} + \epsilon_t; \qquad \epsilon_t \sim \text{Normal}(0, \tau_\zeta)$$

Finally on the regression coefficients (fixed effects) weakly informative prior are specified similarly to the ones presented in (1).

Given that a different spatial resolution has been used across the modelling framework we have summarised it in Table 1, spelling out the reason for each choice to aid clarity.

4.1. Uncertainty Propagation

The fact that our modelling framework is split into two stages means that uncertainty from the predicted NO_2 concentration is not automatically propagated into the health model which could artificially increase the precision of the estimates of the NO_2 effect. To take into account uncertainty we propose to draw J values (e.g. 1,000) from the posterior distribution of NO_2 at the area level obtained from (2) and then to include each $NO_{2B_k tj}$ into the health model

$$\log(\theta_{ktj}) = \gamma_0 + \gamma_{NO_2} NO_{2B_k tj} + \dots \tag{5}$$

which is then run J times. Then the posterior distribution of γ_{NO_2} will be combined across all the runs accounting for the uncertainty.

To evaluate the impact of uncertainty on the air pollution effect estimates we compare this model with the *naive* one, obtained simply plugging in the posterior mean of the NO_2 estimates for each area and time point into the health model.

5. Bayesian inference with INLA and SPDE

INLA (Rue et al., 2009; Blangiardo and Cameletti, 2015) is a computationally efficient alternative to Markov chain Monte Carlo (MCMC) methods, which are usually adopted for Bayesian inference but suffer from computational complexity, especially in case of large datasets characterized by high spatial and/or temporal resolution. INLA performs approximate Bayesian inference for latent Gaussian models by using integrated nested Laplace approximations and its use is now well established in several research fields, including ecology, epidemiology, econometrics and environmental science (Illian et al., 2013; Blangiardo et al., 2013; Musenge et al., 2013; Bilancia and Demarinis, 2014; Carson and Mills Flemming, 2014; Cosandey-Godin et al., 2015; Bivand et al., 2014; Muff et al., 2015; Mtambo et al., 2015; Gómez-Rubio et al., 2015), also thanks to the availability of the `R-INLA` package.

Latent Gaussian models can be represented through hierarchical structures; using the general notation adopted in Blangiardo and Cameletti (2015), at the first stage the model for the data $\boldsymbol{y} = (y_1, \ldots, y_n)$ is defined assuming independence conditionally on the latent field $\boldsymbol{\theta}$ (which includes both fixed and random effects defined in the linear predictor) and on the hyperparameters $\boldsymbol{\psi} = (\psi_1, \ldots, \psi_K)$:

$$\boldsymbol{y} \mid \boldsymbol{\theta}, \boldsymbol{\psi} \sim p(\boldsymbol{y} \mid \boldsymbol{\theta}, \boldsymbol{\psi}) = \prod_{i=1}^{n} p\left(y_i \mid \theta_i, \boldsymbol{\psi}\right).$$

At the second stage, a multivariate Normal prior is assumed on $\boldsymbol{\theta}$ with mean $\mathbf{0}$ and precision matrix $\boldsymbol{Q}(\boldsymbol{\psi})$, i.e. $\boldsymbol{\theta} \mid \boldsymbol{\psi} \sim p(\boldsymbol{\theta} \mid \boldsymbol{\psi}) = \text{Normal}\left(\mathbf{0}, \boldsymbol{Q}(\boldsymbol{\psi})^{-1}\right)$. For a wide range of models we can assume that the components of the latent Gaussian field $\boldsymbol{\theta}$ admit conditional independence, hence the precision matrix $\boldsymbol{Q}(\boldsymbol{\psi})$ is sparse and the latent field $\boldsymbol{\theta}$ is a Gaussian Markov random field (GMRF, Rue and Held, 2005). The sparsity of the precision matrix is crucial for computational benefits, as it allows to use numerical methods for sparse matrices which are faster then the general algorithms for dense matrices. The hierarchical model specification is then completed with a prior for the hyperparameters $\boldsymbol{\psi} \sim p(\boldsymbol{\psi})$.

The INLA algorithm substitutes MCMC simulations with accurate deterministic approximations to the marginal posterior distributions of interest for each element of the parameter and hyperparameter vector, i.e. $p(\theta_i \mid \boldsymbol{y})$ and $p(\psi_k \mid \boldsymbol{y})$. Moreover, as described in Martins et al. (2013), INLA can

provide approximations to the posterior marginals of linear combinations of the latent field defined as $\boldsymbol{\nu} = \boldsymbol{B\theta}$, where matrix $\boldsymbol{B}$ contains the weights defining the linear combination.

When Bayesian inference involves a spatial process defined over a continuous domain (i.e. a GF), it is possible to combine INLA with the Stochastic Partial Differential Equation (SPDE) approach proposed by Lindgren et al. (2011). The strength of SPDE derives from representing a GF with Matérn spatial covariance function as a discrete indexed GMRF, which is characterized by a sparse precision matrix and enjoys computational benefits in terms of fast inference.

This representation is based on a finite combination of piecewise linear functions defined over a triangulation (or mesh) of the domain of interest and with basis weights defined by a GMRF with sparse precision matrix explicitly depending on the Matérn parameters (Simpson et al., 2012a,b). Spatial prediction in a given location belonging to the considered spatial domain is straightforward since SPDE provides the approximation of the entire spatial process; it is just a matter of including in the model the locations where predictions are required as missing values observations (Lindgren and Rue, 2015). For a comprehensive review on the INLA and SPDE approach we refer the reader to Blangiardo et al. (2013) and Blangiardo and Cameletti (2015).

6. Results

First stage model

Running the model presented in (1) on our data and using the mesh with 342 vertexes shown in Figure 5 we obtain the coefficients reported in Table 2: the intercept value, equal to 5.049 on the square root scale, corresponds to a posterior average pollution level of about 25.8 $\mu g/m^3$, after adjustment for covariates. As expected a significant and negative relationship is observed between temperature and NO_2 concentration, while the coefficient of NO_2 baseline level indicates a positive association. The lag one coefficient $a = 0.9782$ shows a strong correlation in time; the spatial range estimate is equal to $\rho = 1.911$ degrees which corresponds to about 210 km, thus denoting a spatial correlation almost null for medium-long distances. Then after performing point-to-area prediction as presented in (2), we obtain predictive distributions of NO_2 concentration for each time point and for each area at the MSOA level; an example of this high-resolution map, is reported in

Figure 6, which displays the posterior mean, posterior 2.5% and 97.5% for December 2011.

Additionally, in order to validate the model we re-run the first stage dropping 10% of the monitoring stations: by comparing predicted and observed values we obtain an average (over stations) correlation index equal to 0.91, an average mean absolute percentage error (MAPE=$\frac{1}{28}\sum_{t=1}^{28}\frac{|\hat{y}_i - y_i|}{y_i}$, Morrison et al., 2016) equal to 0.03 and an average root mean square error given by 0.62. This suggests that the model is able to accurately capture the space-time dynamics.

	mean	0.025quant	0.5quant	0.975quant
β_0	5.0490	3.9140	5.0510	6.1710
β_1	-0.1040	-0.1210	-0.1050	-0.0860
β_2	0.0180	0.0110	0.0180	0.0260
σ_e^2	0.2515	0.2337	0.2513	0.2706
a	0.9782	0.9722	0.9784	0.9832
σ_ω^2	2.7539	1.9980	2.7205	3.6917
ρ	1.9110	1.4580	1.8946	2.4530

Table 2: Posterior estimates (mean and quantiles) of the NO_2 model (first stage).

Second stage model

Including the NO_2 posterior distribution in the health model we obtain the results presented in Table 3: the posterior summary for the regression coefficients are reported for (i) the main model, which takes uncertainty from the first stage into account through re-sampling of NO_2 concentration from its posterior distribution, as presented in (5) and (ii) the *naive* model, which includes only the posterior means of NO_2 from the first stage model. We find a small association between NO_2 and GP prescriptions, with a posterior relative risk of prescribing increasing on average by 0.07% when NO_2 increases of 10 $\mu g/m^3$ (CI95 going from 0.01% to 0.15%). The numbers might seem very small, but this can loosely translate into an additional monthly 31,547 prescriptions across England assuming that NO_2 increases of 10 $\mu g/m^3$ in each MSOA. The confounders show an effect on the outcome: as expected deprivation is associated with prescriptions, with a posterior mean relative risk increasing of almost 60% going from the least deprived (first quartile of IMD) to the most deprived (4th quartile of IMD) areas. Also population structure

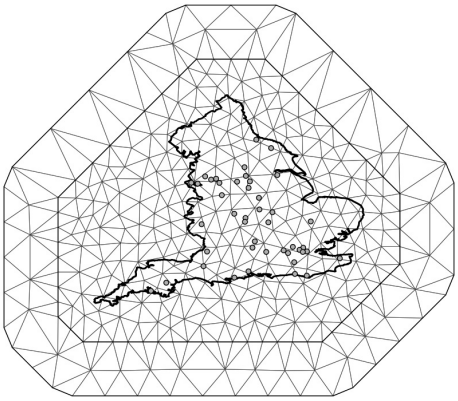

Figure 5: Representation of the triangulation (or mesh) with 342 vertexes used for the SPDE basis function representation of the Matérn Gaussian field. The grey points denote the NO_2 monitoring stations.

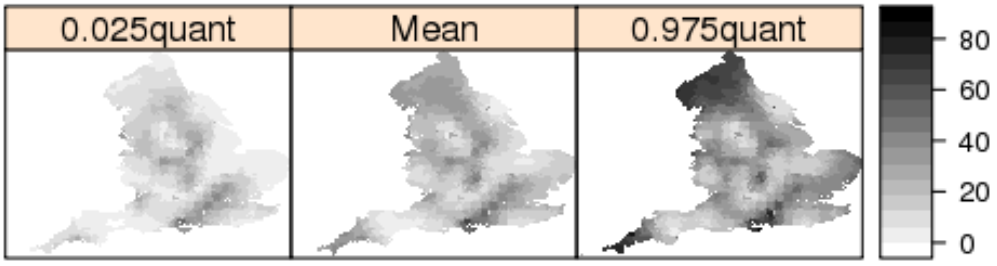

Figure 6: Posterior summaries (2.5% quantile, mean, 0.975% quantile) of NO_2 concentration (in $\mu g/m^3$) at the MSOA level for December 2011.

	With Uncertainty			
	mean	0.025quant	0.5quant	0.975quant
NO_2	1.0007	1.0001	1.0006	1.0015
IMD(q2)	1.1454	1.1443	1.1454	1.1466
IMD(q3)	1.3448	1.3431	1.3448	1.3464
IMD(q4)	1.5886	1.5865	1.5886	1.5907
% male	1.9611	1.9246	1.9610	2.0014
% active pop	0.1597	0.1581	0.1597	0.1613
COPD prev.	35.0624	32.6591	35.0176	37.7483
Asthma prev.	8065.1546	7834.6360	8063.9923	8303.9261
	Without Uncertainty			
	mean	0.025quant	0.5quant	0.975quant
NO_2	1.0010	1.0003	1.0010	1.0014
IMD(q2)	1.1454	1.1443	1.145	1.1465
IMD(q3)	1.3449	1.3433	1.3449	1.3465
IMD(q4)	1.5886	1.5865	1.5886	1.5908
% male	1.9618	1.9242	1.9616	1.9989
% active pop	0.1597	0.1580	0.1597	0.1614
COPD prev.	35.0163	32.4203	35.0578	37.7270
Asthma prev.	8069.7698	7849.0205	8069.3956	8299.9460

Table 3: Posterior estimates (mean and CI95) of the relative risks in the health model (second stage). The top part of the table shows the results from the model which takes into account uncertainty on the NO_2 concentration estimates from the first stage model; the bottom part of the table presents the results of the *naive* analysis, plugging the posterior mean of NO_2 concentration estimates only.

presents an association with prescriptions, with a posterior mean relative risk equal to 0.16 for active population versus older/younger patients and of 1.96 for males compared to females. Finally areas where the prevalence of COPD and asthma is higher experience higher rates of prescriptions as expected (posterior mean relative risk equal to 35.062 and 8065.154 respectively).

Comparing the results reported above to the ones for the *naive* model shows (i) a change in the NO_2 posterior distribution, which is narrower and has a mean further away from zero (posterior mean relative risk suggesting a 0.1% increase in the prescription rate when NO_2 increases of 10 $\mu g/m^3$ and a credibility intervals going from 0.03% to 0.14%); (ii) stable results for the confounders. The hyperparameter ϕ shows that about 70% of the

variability is explained by the spatial component $\boldsymbol{u}^* = \{u_1^*, \ldots, u_{211}^*\}$ in both the model specifications (with and without uncertainty, see Figure 7) and Figure 8 presents the map of the spatial residual ($\exp(u_c^* + v_c)$), suggesting the presence of spatial variation.

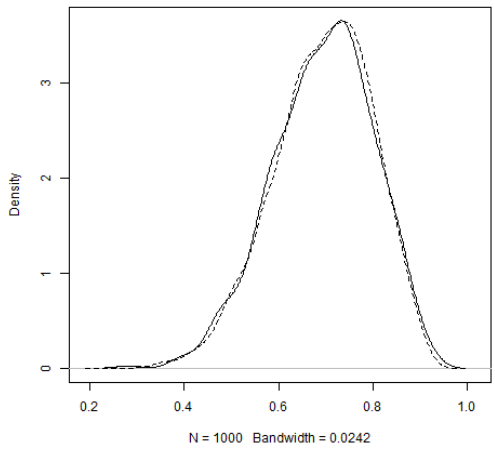

Figure 7: Posterior distributions of the hyperparameter ϕ for the model with and without uncertainty (dashed and solid line respectively). They show a similar behavior, with about 70% of the variability explained by the spatial component $\boldsymbol{u}^*$.

7. Discussion

In this paper we have developed a two stage modelling framework to evaluate the effect of NO_2 concentration on $\beta 2$-agonist to control chronic respiratory diseases like asthma and COPD in a primary care perspective, i.e. considering the general population instead of focussing on severe cases only (i.e. using hospital admissions or mortality registries). Similarly to the recent literature on air pollution statistical modelling we have considered a Bayesian spatio-temporal specification to account for spatial and temporal misalignment between pollutant concentration data, which are available at a finite number of monitoring stations on a daily basis, and disease data, represented by counts over spatial units at a monthly resolution.

The Integrated Nested Laplace Approximations approach (INLA) has proven to be a faster alternative to MCMC yet providing accurate results;

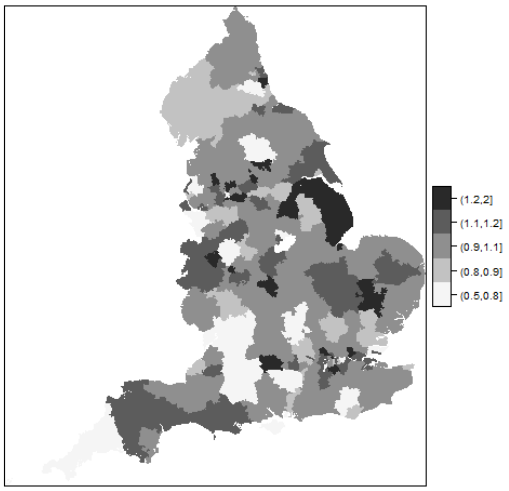

Figure 8: Posterior distribution of the spatial random effects $\exp(u_c^* + v_c)$ for the model with uncertainty. The map shows the presence of spatially structured variation, which is in line with the posterior distribution of the hyperparameter ϕ.

INLA coupled with the Stochastic Partial Differential Equation (SPDE) strategy means that also continuous spatial domains can benefit from the sparsity of precision matrices which results in reduced computational burden making possible to work with fine spatio-temporal resolutions. In our case the point-to-point and point-to-area prediction involved 690 grid points and 6790 areas replicated over 28 time points, a highly computationally intensive task which can be tackled in a single `R-INLA` routine, performing at the same time parameter estimation and spatial prediction. In addition the specification of the modified BYM prior relaxes the assumption that the spatially structured and unstructured random effects are independent, and provides a more interpretable way of comparing the relative impact of the two random effects on the total variability through the ϕ hyperparameter.

Similarly to Lee and Shaddick (2010), we move away from the standard public health approach which summarizes the (posterior) distribution of the pollutant via the mean or median and plugs it in the health model: our modeling approach feeds the entire NO_2 posterior predictive distributions for each area into the small area health model, thus accounting for the uncertainty intrinsic in the concentration estimates in the health model. This is

a simple solution to take into account that the exposure level predicted at the first-stage, and included in the health model as covariate, do not necessarily represent the true area level exposure. Alternatively, it would be possible to refer to the measurement error modeling framework (see e.g. Gryparis et al., 2009; MacNab, 2009; Szpiro et al., 2011; Lopiano et al., 2013; Szpiro and Paciorek, 2013) and define an ecological regression model accounting for errors in covariates. In a fully Bayesian framework the natural approach would consist in a joint model of exposure and health, which would allow to propagate properly all the uncertainty sources (due to spatial misalignment, measurement error, etc.). However this would require careful thinking into allowing/blocking the impact of the outcome from the health model on the prediction of the pollutant; in addition this approach raises computational issues which are beyond the scope of this paper and will be explored the future. We have compared our model with the *naive* formulation which does not take uncertainty into account and have found as expected a wider posterior distribution and a posterior mean shifted towards zero when uncertainty is considered.

A limitation of our approach is that by default in `R-INLA` the posterior marginals are obtained for each MSOA, while the joint posterior distribution would be normally available through a MCMC algorithm. This means that the NO_2 sampling is done independently for each area and time point. It is in theory possible to account for the spatio-temporal structure starting from the joint posterior correlation matrix and then sampling using a Gaussian approximation, but this would increase substantially the computational burden given the number of areas and time points we are considering in this work. To understand the impact of independent sampling on the spatial correlation, we computed Moran's autocorrelation index for each time point and posterior sample and obtained values between 0.692 and 0.774, thus suggesting that some degree of spatial correlation is maintained. Temporal correlation was studied through the correlograms and it was found that at the first lag the absolute serial correlation is on average equal to 0.534 with 75% of the values being greater than 0.4. Thus, it seems reasonable to conclude that the NO_2 spatio-temporal correlation is not completely lost even when sampling from the posterior marginal predictive distributions. Recently a new function has been made available in the `R-INLA` package for sampling from the joint posterior distribution, but it is still at an experimental stage and its behaviour in the present context needs to be tested with an exhaustive simulation study, which is the object of a current research project.

We need to stress that given the nature of the available prescription data, which are aggregated at the GP level not even disaggregated for age/sex, we cannot make inference at the individual level or link the data with hospital admissions or mortality registries to follow the individuals from primary to secondary care; nevertheless we think that this is an important contribution at the population level to understand the impact that air pollution might have in new cases or in exacerbating asthma and COPD conditions. This analysis could be linked to a proper health economic evaluation to provide policy makers with figures related to additional NHS spending (or saving) for different air pollution scenarios (for instance what would be the impact of implementing the congestion charge in several large cities in England).

8. Acknowledgements

We acknowledge the E-OBS dataset from the EU-FP6 project ENSEMBLES (http://ensembles-eu.metoffice.com) and the data providers in the ECAD project (http://www.ecad.eu). We would like to thank Dr John Gulliver for providing the NO_2 2009 baseline data and Dr Gianluca Baio for commenting on the manuscript.

All the authors have been supported by the FIRB Project StEPhI (project no. RBFR12URQJ, http://stephiproject.it/) provided by the Italian Ministry for Education, University and Research.

References

Atkinson, R. W., Mills, I. C., Walton, H. A., Anderson, H. R., 2014. Fine particle components and health - systematic review and meta-analysis of epidemiological time series studies of daily mortality and hospital admissions. Journal of Exposure Science and Environmental Epidemiology 25 (2), 208–214.

Berrocal, V., Gelfand, A., Holland, D., 2010a. A spatio-temporal downscaler for output from numerical models. Journal of Agricultural, Biological, and Environmental Statistics 15 (2), 176–197.

Berrocal, V. J., Gelfand, A. E., Holland, D. M., 2010b. A spatio-temporal downscaler for output from numerical models. Journal of Agricultural, Biological, and Environmental Statistics 15 (2), 176–197.

Besag, J., York, J., Mollié, A., 1991. Bayesian Image Restoration with Two Applications in Spatial Statistics. The Annals of the Institute of Statistics and Mathematics 43 (1), 1 – 59.

Bilancia, M., Demarinis, G., 2014. Bayesian scanning of spatial disease rates with integrated nested Laplace approximation (INLA). Statistical Methods and Applications 23 (1), 71–94.

Bivand, R. S., Gómez-Rubio, V., Rue, H., 2014. Approximate Bayesian inference for spatial econometrics models. Spatial Statistics 9, 146–165.

Blangiardo, M., Cameletti, M., 2015. Spatial and Spatio-temporal Bayesian Models with `R-INLA`. Wiley.

Blangiardo, M., Cameletti, M., Baio, G., Rue, H., 2013. Spatial and spatio-temporal models with `R-INLA`. Spatial and Spatio-temporal Epidemiology 4, 33 – 49.

Brook, R. D., Rajagopalan, S., Pope, C. A., Brook, J. R., Bhatnagar, A., Diez-Roux, A. V., Holguin, F., Hong, Y., Luepker, R. V., Mittleman, M. A., Peters, A., Siscovick, D., Smith, S. C., Whitsel, L., Kaufman, J. D., 2010. Particulate matter air pollution and cardiovascular disease: an update to the scientific statement from the American Heart Association. Circulation 121, 12331–2378.

Brunekreef, B., Holgate, S. T., 2002. Air pollution and health. The lancet 360 (9341), 1233–1242.

Cameletti, M., Ignaccolo, R., Bande, S., 2011. Comparing spatio-temporal models for particulate matter in Piemonte. Environmetrics 22 (8), 985–996.

Cameletti, M., Lindgren, F., Simpson, D., Rue, H., 2013. Spatio-temporal modeling of particulate matter concentration through the SPDE approach. AStA Advances in Statistical Analysis 97 (2), 109–131.

Carslaw, D., Ropkins, K., 2015. openair: Open-source tools for the analysis of air pollution data. `R` package version 1.5.

Carslaw, D. C., Ropkins, K., 2012. openair - An `R` package for air quality data analysis. Environmental Modelling & Software 27-28 (0), 52–61.

Carson, S., Mills Flemming, J., 2014. Seal encounters at sea: A contemporary spatial approach using `R-INLA`. Ecological Modelling 291, 175–181.

Clayton, T. C., Thompson, M., Meade, T. W., 2008. Recent respiratory infection and risk of cardiovascular disease: case-control study through a general practice database. European heart journal 29 (1), 96–103.

Cocchi, D., Greco, F., Trivisano, C., 2007. Hierarchical space-time modelling of PM_{10} pollution. Atmospheric environment 41, 532–542.

Cosandey-Godin, A., Teixeira Krainski, E., Worm, B., Mills Flemming, J., 2015. Applying Bayesian spatio-temporal models to fisheries bycatch in the Canadian Arctic. Canadian Journal of Fisheries and Aquatic Sciences 72 (2), 186–197.

Cressie, N., Wikle, C., 2011. Statistics For Spatio- Temporal Data. Wiley.

Dockery, D. W., Pope, C. A., Xu, X., Spengler, J. D., Ware, J. H., Fay, M. E., Ferris Jr, B. G., Speizer, F. E., 1993. An association between air pollution and mortality in six US cities. New England journal of medicine 329 (24), 1753–1759.

Fassò, A., Finazzi, F., 2011. Maximum likelihood estimation of the dynamic coregionalization model with heterotopic data. Environmetrics 22 (6), 735–748.

Fuentes, M., Raftery, A., 2005. Model Evaluation and Spatial Interpolation by Bayesian Combination of Observations with Outputs from Numerical Models. Biometrics 61 (1), 36–45.

Gelfand, A., Diggle, P., Fuentes, M., Guttorp, P. (Eds.), 2010. Handbook of Spatial Statistics. Chapman & Hall.

Gómez-Rubio, V., Cameletti, M., Finazzi, F., 2015. Analysis of massive marked point patterns with stochastic partial differential equations. Spatial Statistics 14, 179–196.

Gotway, C., Young, L., 2002. Combining incompatible spatial data. Journal of the American Statistical Association 97 (458), 632–648.

Gryparis, A., Paciorek, C. J., Zeka, A., Schwartz, J., Coull, B. A., 2009. Measurement error caused by spatial misalignment in environmental epidemiology. Biostatistics 10 (2), 258–274.

Gulliver, J., de Hoogh, K., Hansell, A., Vienneau, D., 2013. Development and Back-Extrapolation of NO2 Land Use Regression Models for Historic Exposure Assessment in Great Britain. Environmental Science & Technology 47 (14), 7804–7811.

Hansell, A., Hollowell, J., Nichols, T., McNiece, R., Strachan, D., 1999. Use of the General Practice Research Database (GPRD) for respiratory epidemiology: a comparison with the 4th Morbidity Survey in General Practice (MSGP4). Thorax 54 (5), 413–419.

Haylock, M., Hofstra, N., Klein Tank, A., Klok, E., Jones, P., New, M., 2008. An European daily high-resolution gridded data set of surface temperature and precipitation for 1950-2006. Journal of Geophysical Research: Atmospheres (1984-2012) 113 (D20).

Howie, J., Richardson, I., Gill, G., Durno, D., 1971. Respiratory illness and antibiotic use in general practice. The Journal of the Royal College of General Practitioners 21 (112), 657.

Huang, G., Lee, D., Scott, M., 2015. An integrated Bayesian model for estimating the long-term health effects of air pollution by fusing modelled and measured pollution data: a case study of nitrogen dioxide concentrations in Scotland. Spatial and Spatio-temporal Epidemiology 14-15, 63–74.

Illian, J. B., Martino, S., Sørbye, S. H., Gallego-Fernández, J. B., Zunzunegui, M., Esquivias, M. P., Travis, J. M. J., 2013. Fitting complex ecological point process models with integrated nested Laplace approximation. Methods in Ecology and Evolution 4 (4), 305–315.

Jick, S. S., Kaye, J. A., Vasilakis-Scaramozza, C., Rodríguez, L. A. G., Ruigómez, A., Meier, C. R., Schlienger, R. G., Black, C., Jick, H., 2003. Validity of the general practice research database. Pharmacotherapy: The Journal of Human Pharmacology and Drug Therapy 23 (5), 686–689.

Katz, N., Panas, L., Kim, M., Audet, A. D., Bilansky, A., Eadie, J., Kreiner, P., Paillard, F. C., Thomas, C., Carrow, G., 2010. Usefulness of prescription monitoring programs for surveillance analysis of schedule II opioid

prescription data in Massachusetts, 1996-2006. Pharmacoepidemiology and drug safety 19 (2), 115–123.

Künzli, N., 2012. Is air pollution of the 20th century a cause of current asthma hospitalisations? Thorax 67 (1), 2–3.

Lanki, T., Pekkanen, J., Aalto, P., Elosua, R., Berglind, N., D'Ippoliti, D., Kulmala, M., Nyberg, F., Peters, A., Picciotto, S., Salomaa, V., Sunyer, J., Tiittanen, P., von Klot, S., Forastiere, F., 2006. Associations of traffic related air pollutants with hospitalisation for first acute myocardial infarction: the HEAPSS study. Occupational and environmental medicine 63 (12), 844–851.

Lasinio, G. J., Mastrantonio, G., Pollice, A., 2013. Discussing the big n problem. Statistical Methods & Applications 22 (1), 97–112.

Laurent, O., Pedrono, G., Filleul, L., Segala, C., Lefranc, A., Schillinger, C., Rivière, E., Bard, D., 2009. Influence of socioeconomic deprivation on the relation between air pollution and β-agonist sales for asthma. Chest Journal 135 (3), 717–723.

Lawson, A., Choi, J., Cai, B., Hossain, M., Kirby, R., Liu, J., 2012. Bayesian 2-Stage Space-Time Mixture Modeling With Spatial Misalignment of the Exposure in Small Area Health Data. Journal of Agricultural, Biological, and Environmental Statistics 17 (3), 417–441.

Lee, D., Sarran, C., 2015. Controlling for unmeasured confounding and spatial misalignment in long-term air pollution and health studies. Environmetrics, 477–487.

Lee, D., Shaddick, G., 2010. Spatial modeling of air pollution in studies of its short-term health effects. Biometrics 66 (4), 1238–1246.

Lindgren, F., Rue, H., 2015. Bayesian Spatial Modelling with `R-INLA`. Journal of Statistical Software 63 (19), 1–25.

Lindgren, F., Rue, H., Lindström, J., 2011. An explicit link between Gaussian fields and Gaussian Markov random fields: the stochastic partial differential equation approach. Journal of the Royal Statistical Society: Series B 73 (4), 423–498.

Lopiano, K. K., Young, L. J., Gotway, C. A., 2013. Estimated generalized least squares in spatially misaligned regression models with berkson error. Biostatistics 14 (4), 737–751.

MacNab, Y. C., 2009. Bayesian multivariate disease mapping and ecological regression with errors in covariates: Bayesian estimation of dalys and 'preventable' dalys. Statistics in Medicine 28, 13691385.

MacNab, Y. C., 2011. On gaussian markov random fields and bayesian disease mapping. Statistical Methods in Medical Research 20, 49–68.

Martins, T. G., Simpson, D., Lindgren, F., Rue, H., 2013. Bayesian computing with INLA: New features. Computational Statistics & Data Analysis 67, 68–83.

Masoli, M., Fabian, D., Holt, S., Beasley, R., 2004. The global burden of asthma: executive summary of the GINA dissemination committee report. Allergy 59 (5), 469–478.

Morrison, J., Shaddick, G., Henderson, S., Buckeridge, D., 2016. A latent process model for forecasting multiple time series in environmental public health surveillance. Statistics in medicine –, –, to appear.

Moth, G., Vedsted, P., Schiøtz, P. O., 2007. Identification of asthmatic children using prescription data and diagnosis. European journal of clinical pharmacology 63 (6), 605–611.

Mtambo, O., Masangwi, S., Kazembe, L., 2015. Spatial quantile regression using INLA with applications to childhood overweight in Malawi. Spatial and Spatio-temporal Epidemiology 13, 7–14.

Muff, S., Riebler, A., Held, L., Rue, H., Saner, P., 2015. Bayesian analysis of measurement error models using integrated nested Laplace approximations. Journal of the Royal Statistical Society: Series C 64 (2), 231–252.

Musenge, E., Chirwa, T. F., Kahn, K., Vounatsou, P., 2013. Bayesian analysis of zero inflated spatiotemporal HIV/TB child mortality data through the INLA and SPDE approaches: Applied to data observed between 1992 and 2010 in rural North East South Africa. International Journal of Applied Earth Observation and Geoinformation 22 (0), 86 – 98.

Naureckas, E. T., Dukic, V., Bao, X., Rathouz, P., 2005. Short-acting β-agonist prescription fills as a marker for asthma morbidity. Chest Journal 128 (2), 602–608.

Osborn, D. P., Levy, G., Nazareth, I., Petersen, I., Islam, A., King, M. B., 2007. Relative risk of cardiovascular and cancer mortality in people with severe mental illness from the United Kingdom's general practice research database. Archives of general psychiatry 64 (2), 242–249.

Petersen, I., Johnson, A., Islam, A., Duckworth, G., Livermore, D., Hayward, A., 2007. Protective effect of antibiotics against serious complications of common respiratory tract infections: retrospective cohort study with the UK general practice research database. BMJ 335 (7627), 982.

Prescribing and Primary Care Health and Social Care Information Centre, 2014. Prescriptions dispensed in the Community. England 2003-2013. Tech. rep., Health & Social Care Information Centre (HSCIC), http://www.hscic.gov.uk/catalogue/PUB14414.

Rue, H., Held, L., 2005. Gaussian Markov Random Fields. Theory and Applications. Chapman & Hall.

Rue, H., Martino, S., Chopin, N., 2009. Approximate Bayesian inference for latent Gaussian models by using integrated nested Laplace approximations. Journal of the Royal Statistical Society: Series B 2 (71), 1–35.

Rushworth, A., Lee, D., Mitchell, R., 2014. A spatio-temporal model for estimating the long-term effects of air pollution on respiratory hospital admissions in Greater London. Spatial and spatio-temporal epidemiology 10, 29–38.

Sahu, S., 2011. Hierarchical Bayesian models for space-time air pollution data. In: Rao, C. (Ed.), Handbook of Statistics - Time Series Analysis, Methods and Applications. Vol. 30 of Handbook of Statistics. Elsevier Publishers, Holland.

Sahu, S., Gelfand, A., Holland, D., 2010. Fusing point and areal level space-time data with application to wet deposition. Journal of the Royal Statistical Society: Series C 59 (1), 77–103.

Schikowski, T., Sugiri, D., Ranft, U., Gehring, U., Heinrich, J., Wichmann, H.-E., Kramer, U., 2005. Long-term air pollution exposure and living close to busy roads are associated with copd in women. Respiratory Research 6 (1), 152.

Schwartz, J., Marcus, A., 1990. Mortality and air pollution in London: a time series analysis. American Journal of Epidemiology 131 (1), 185–194.

Simpson, D., Lindgren, F., Rue, H., 2012a. In order to make spatial statistics computationally feasible, we need to forget about the covariance function. Environmetrics 23 (1), 65–74.

Simpson, D., Lindgren, F., Rue, H., 2012b. Think continuous: Markovian gaussian models in spatial statistics. Spatial Statistics 1, 16–29.

Simpson, D., Rue, H., Martins, T., Riebler, A., Sorbye, S., 2015. Penalising model component complexity: A principled, practical approach to constructing priors. ARXIV, 1–45.
URL http://arxiv.org/pdf/1403.4630.pdf

Sofianopoulou, E., Rushton, S. P., Diggle, P. J., Pless-Mulloli, T., 2013. Association between respiratory prescribing, air pollution and deprivation in primary health care. Journal of Public Health 35 (4), 502–509.

Szpiro, A. A., Paciorek, C. J., 2013. Measurement error in two-stage analyses, with application to air pollution epidemiology. Environmetrics 24 (8), 501–517.

Szpiro, A. A., Sheppard, L., Lumley, T., 10 2011. Efficient measurement error correction with spatially misaligned data. Biostatistics 12 (4), 610–623.

Vegni, F. E., Castelli, B., Auxilia, F., Wilkinson, P., 2005. Air pollution and respiratory drug use in the city of Como, Italy. European journal of epidemiology 20 (4), 351–358.

Vos, T., Barber, R. M., Bell, B., Bertozzi-Villa, A., Biryukov, S., Bolliger, I., et. al, 2015. Global, regional, and national incidence, prevalence, and years lived with disability for 301 acute and chronic diseases and injuries in 188 countries, 1990–2013: a systematic analysis for the global burden of disease study 2013. The Lancet 386 (9995), 743–800.

WHO, 2012. Prevention and control of noncommunicable diseases: Guidelines for primary health care in low resource settings. World Health Organization, http://www.who.int/nmh/publications/phc2012/en/.

Zidek, J. V., Le, N. D., Liu, Z., 2011. Combining data and simulated data for space–time fields: application to ozone. Environmental and Ecological Statistics 19 (1), 37–56.